PHYSICAL REVIEW B **73**, 180404(R) (2006)

Dynamical mean-field study of the ferromagnetic transition temperature of a two-band model for colossal magnetoresistance materials

F. Popescu,[1] C. Şen,[1,2] and E. Dagotto[3,4]
[1]*Department of Physics, Florida State University, Tallahassee, Florida 32306, USA*
[2]*National High Magnetic Field Laboratory, Tallahassee, Florida 32310, USA*
[3]*Department of Physics and Astronomy, University of Tennessee, Knoxville, Tennessee 37996, USA*
[4]*Condensed Matter Sciences Division, Oak Ridge National Laboratory, Oak Ridge, Tennessee 32831, USA*
(Received 17 March 2006; revised manuscript received 19 April 2006; published 24 May 2006)

The ferromagnetic transition temperature (T_C) of a two-band double-exchange (DE) model for colossal magnetoresistance materials is studied using dynamical mean-field theory in wide ranges of coupling constants, hopping parameters, and carrier densities. The results are shown to be in good agreement with Monte Carlo simulations. When the bands overlap, the value of T_C is found to be much larger than in the one-band case, for all values of the chemical potential within the energy overlap interval. A nonzero off-diagonal hopping produces an additional boost of T_C, showing the importance of these terms, as well as the concomitant use of multiband models, to increase the critical temperatures in DE-based theories.

DOI: 10.1103/PhysRevB.73.180404 PACS number(s): 75.47.Lx, 71.27.+a, 71.30.+h

Colossal magnetoresistance (CMR) rare-earth perovskites have attracted considerable attention due to their rich magnetic and structural phase transitions.[1] The CMR effect, namely an extremely large drop in resistivity caused by a magnetic field, occurs at the transition between a low-temperature ferromagnetic (FM)-metallic ground state and a high-temperature paramagnetic-insulating phase, i.e., near transition temperature (T_C). A basic aspect of CMR physics is that the mobile carriers (Mn e_g-symmetry electrons) are strongly coupled ferromagnetically to localized spins (Mn t_{2g}-symmetry electrons). The electron motion influences the core spin's alignment leading to ferromagnetism. The basic model used to describe CMR materials is the double-exchange (DE) model,[2] formulated with one localized spin per site coupled to mobile carriers via a Hund's coupling J much larger than the hopping amplitude t (Ref. 3). While DE ideas explain qualitatively the ferromagnetism, much of the CMR physics is still under debate.[4,5] This is in part caused by the absence of fully reliable many-body techniques to study the complicated DE models applied to CMR compounds. Despite a considerable effort carried out within dynamical mean-field theory (DMFT) in the context of one-band models for CMR (Ref. 6), the realistic case of two active bands has received much less attention since its analysis is far more difficult. Only MC and static mean-field approximations have been applied to the realistic multiband problem,[5] the DMFT treatment being notoriously absent.

In this paper the DMFT method is applied to the analysis of T_C of a two-band model for CMR materials. Its results are contrasted against Monte Carlo (MC) simulations and found to be in good agreement. Besides this nontrivial technically DMFT+MC contribution, we also unveil the key role of the *off-diagonal* hopping amplitudes to increase the critical FM temperature. This effect, which, to the best of our knowledge has not yet been discussed in literature, may lead to creative procedures to boost T_C in real materials. Our DMFT study is general, with two $s=1/2$ active bands, arbitrary couplings, hoppings, and carrier densities p.

The DE Hamiltonian for the two-orbital model is

$$\mathcal{H} = -\sum_{ll',\langle ji\rangle\alpha} (t_{ll'} c^{\dagger}_{l',j\alpha} c_{l,i\alpha} + \text{H.c.}) - 2\sum_{l,i} J_l \mathbf{S}_i \cdot \mathbf{s}_{l,i}, \quad (1)$$

where l,l' $(=1,2)$ are the e_g-orbital indexes, i,j label the sites, $c_{l,i\alpha}$ destroys an electron at site i in the orbital l, $\mathbf{s}_{l,i} = c^{\dagger}_{l,i\beta}(\boldsymbol{\sigma}_{\beta\alpha}/2)c_{l,i\alpha}$ is the electronic spin ($\hat{\boldsymbol{\sigma}}$=Pauli vector), α and β are spin indexes, $\mathbf{S}_i$ is the spin of the local moment at site i, assumed here classical ($\mathbf{S}_i = S\mathbf{m}_i$, where $\mathbf{m}_i$ is a randomly orientated unit vector), and J_l is the coupling between the core spin and the conduction electrons of orbital l. While for $l=l'$ we refer to t_{ll} as the direct-orbital hopping ($\equiv t_l$), for $l \neq l'$ the off-diagonal $t_{ll'}$ is referred to as the "interorbital" hopping ($t_{ll'} = t_{l'l}$). The active orbital bands couple through the simultaneous scattering of carriers on the same core spin, as well as through the exchange of carriers via the off-diagonal hopping. While the first coupling clearly causes an *increase* in T_C when the bands overlap within the same energy interval, namely when J_l are closed, the electron exchange among bands is *also* shown to induce higher T_C even when the J_l's are very different.

The inclusion of other terms, such as the antiferromagnetic exchange J_{AF} among core spins and/or the cooperative Jahn–Teller phonons, will need a sophisticated "cluster" DMFT where at least some short-distance effects are considered. For this reason, this study using the DMFT on a two-band model focuses on the simplest case where only the FM phase is relevant, the competition with other phases being left for future studies.

DMFT results. Within DMFT, the self-energy is momentum independent; $\Sigma(\mathbf{p}, i\omega_n) \to \Sigma(i\omega_n)$ [$\omega_n = (2n+1)\pi T$ are the Matsubara frequencies]. Hence, the information about the hopping of carriers on and off lattice sites is carried by the bare Green's function $\mathcal{G}_0(i\omega_n)$. Within one-band models, the local effective action $\mathcal{S}_{eff}(\mathbf{m})$ defined by $\mathcal{G}_0$ is quadratic in the Grassman variables.[6,7] Hence, the full Green's function $\mathcal{G}$ can be solved by integration with the result: $\langle \mathcal{G}(i\omega_n)\rangle = \langle [\mathcal{G}_0^{-1}(i\omega_n) + J\mathbf{S}\mathbf{m}\hat{\sigma}]^{-1}\rangle$ (Refs. 6 and 8). If two orbital bands are active, then one rewrites the average above for each

band, $\langle \mathcal{G}_l(i\omega_n)\rangle = \langle [\mathcal{G}_{0,l}^{-1}(i\omega_n) + J_l \mathbf{S}_l \mathbf{m} \hat{\sigma}]^{-1}\rangle$, and solve the equations for the coupled Green's functions, $\langle \mathcal{G}_{0,l}^{-1}(i\omega_n)\rangle = z_n - t_l^2 \langle \mathcal{G}_l(i\omega_n)\rangle - t_{ll'}^2 \langle \mathcal{G}_{l'}(i\omega_n)\rangle$ $(l \neq l')$, on a Bethe lattice with a semicircular noninteracting density of states $(\mathrm{DOS})_l(\omega) = \mathrm{Re}\sqrt{4t_l^2 - \omega^2}/2\pi t_l^2$, where $z_n = i\omega_n + \mu$ (μ=chemical potential). $t_{ll'}$ carries in $\mathcal{G}_{0,l}$ the information about the second band l' through $\mathcal{G}_{l'}$. To find T_C, we parametrize $\mathcal{G}_{0,l}^{-1}$ as $\mathcal{G}_{0,l}^{-1}(i\omega_n) = [z_n + R_l(i\omega_n)]\hat{\mathbf{1}} + Q_l(i\omega_n)\hat{\boldsymbol{\sigma}}_z$, and linearize $\mathcal{G}_{0,l}^{-1}$ with order parameter M (Ref. 8). Up to first order in M,

$$R_l = -t_l^2 \frac{B_l}{B_l^2 - J_l^2} - t_{ll'}^2 \frac{B_{l'}}{B_{l'}^2 - J_{l'}^2}, \tag{2}$$

where $B_l(i\omega_n) = z_n + R_l(i\omega_n)$. A similar equation for $R_{l'}$ $(l' \neq l)$ can be obtained by interchanging the band indexes $l \rightarrow l'$. Despite the extreme complexity of Eqs. (2), we managed to perform analytical calculations to decouple the equations set and to obtain separate equations for R_l $(l=1,2)$. The polynomial coefficients of the ninth-order equations for R_l, which are solved numerically, are combinations of all parameters of the model, i.e., couplings and hoppings (not reproduced because of their size). For $t_{ll'}=0$, the ninth-order equations reduce to the third-order ones: $R_l^3 + 2z_n R_l^2 + (z_n^2 + t_l^2 - J_l^2)R_l + z_n t_l^2 = 0$. At $\mu=0$ and with the substitution $i\omega_n \rightarrow \omega$, Eq. (2) gives the interacting electronic DOS_l at $T=0$ (Ref. 9). If $t_{ll'} \neq 0$, then, besides its own parameters t_l and J_l, DOS_l depends also on the parameters characterizing the other band l', i.e., $t_{l'}$ and $J_{l'}$, this interplay of parameters describing the coupling of bands. The obtained equation for $Q_l(i\omega_n)$,

$$Q_l = t_l^2 \frac{J_l M + Q_l}{B_l^2 - J_l^2} + t_{ll'}^2 \frac{J_{l'} M + Q_{l'}}{B_{l'}^2 - J_{l'}^2} + t_l^2 \frac{2J_l^2 Q_l}{3(B_l^2 - J_l^2)^2} + t_{ll'}^2 \frac{2J_{l'}^2 Q_{l'}}{3(B_{l'}^2 - J_{l'}^2)^2}, \tag{3}$$

leads us to an implicit expression for T_C in the form

$$-\frac{4}{3}\sum_{n=0}^{\infty} \frac{\sum_l t_l^2 J_l^2 (B_l^2 - J_l^2)^2 + 2t_{ll'}^2 \prod_l J_l (B_l^2 - J_l^2) - (t_l^2 t_{l'}^2 - t_{ll'}^4)\sum_l J_l^2 (B_l^2 - J_l^2/3)}{\prod_l (B_l^2 - J_l^2)^2 - \sum_l t_l^2 (B_l^2 - J_l^2/3)(B_{l'}^2 - J_{l'}^2)^2 + (t_l^2 t_{l'}^2 - t_{ll'}^4)\prod_l (B_l^2 - J_l^2/3)} = 1, \tag{4}$$

where above, if $l=1$ (2), then $l'=2$ (1). At $t_{ll'}=0$, Eq. (4) reduces to

$$\sum_{l=1}^{2}\sum_{n=0}^{\infty} \frac{-2t_l^2 J_l^2}{3(B_l^2 - J_l^2)^2 - 3t_l^2 (B_l^2 - J_l^2) - 2t_l^2 J_l^2} = 1, \tag{5}$$

where B_l satisfies $B_l^3 - z_n B_l^2 + (t_l^2 - J_l^2)B_l + z_n J_l^2 = 0$. We tested Eqs. (4) and (5) in several cases: (1) at $t_2 = t_{12} = 0$ and $J_2 = 0$ we recovered the one-band model results reported in Ref. 10; (2) at $t_2 = t_{12} = 0$, $J_2 = 0$, and $J_1 \rightarrow \infty$, the results of Ref. 7 are reproduced. Details on the calculations above will be published elsewhere. From Eq. (4), the T_C contained in the Matsubara frequencies was extracted numerically. Equation (5) predicts an increase in T_C only for the values of μ within the energy overlap interval.

In Fig. 1(a), the $\mathrm{DOS}_l(\omega)$ at $J_1/t_1 = 25$ and $J_2/t_2 = 15$ is shown for several $t_{ll'}$. Our J_l/t_l are much larger than both the value $(J_l/t_l)_{\min} \approx 1.4$ that corresponds to the electron and hole bands formation, and the value $J/t = 8$ considered in the one-band model large enough to capture properly the FM features of CMRs (Ref. 11). Thus, the electron bands are centered at $\omega_1^- = -25$ and $\omega_2^- = -15$, respectively (the hole bands, centered at $\omega_1^+ = 25$ and $\omega_2^+ = 15$ due to the electron-hole symmetry, are not shown here for simplicity). For clarity, we plotted $\mathrm{DOS}_2(\omega)$ with a reversed sign. Since $|J_1/t_1 - J_2/t_2| \gg 1$, the bands occupy different energy intervals. Hence, each band gives its own contribution to T_C [Fig. 1(b)]. At $t_{ll'}=0$ the bands are fully decoupled, and the values of T_C match the results of the one-band model for all p's. However, if $t_{ll'} \neq 0$, then the carriers are allowed to hop between the bands and, thus, they can belong simultaneously to both bands. This leads to an increase in the effective number of interacting electrons of each active band. As shown in Fig. 1(a), due to the transfer of electrons among bands, in $\mathrm{DOS}_l(\omega)$ a new region occupied by the interacting electrons builds up within the interval of energies occupied by the $\mathrm{DOS}_{l'}(\omega)$. At $t_{ll'} = t_l$, the effective number of interacting electrons within each energy interval becomes twice as large. Thus, the T_C for all p corresponding to μ within each energy interval, is almost twice larger than in the one-band case [Fig. 1(b)]. Conversely, when the J_l's are similar the coupling of bands is strong enough to lead to a deviation from the semicircular form, especially when $t_{ll'} \sim |J_l - J_{l'}|$ [Fig. 1(c)]. If the bands partially overlap, a hump develops in T_C at all p corresponding to μ within the energy overlap interval [Fig. 1(d)].

In Fig. 2(a), the total interacting $\mathrm{DOS}(\omega)$ (Ref. 9) at $t_1 = 1$, $t_2 = 1/3 \sim 0.33$ is shown, for different $t_{ll'}$ in the case when the bands fully overlap $(J_1/J_2 = 1)$. The electron exchange effect not only increases the effective number of interacting electrons in each band, but also extends the energy region occupied by the bands. However, the total number of interacting electrons does not change, the bands being fully filled for $p=2$. While at $t_{12}=0$ [Eq. (5)] the increase in T_C is due to the overlap of bands [short-dashed curve in Fig. 2(b)], when $t_{ll'} \neq 0$ [see Eq. (4)] the exchange effect further boosts T_C [Fig. 2(b)].

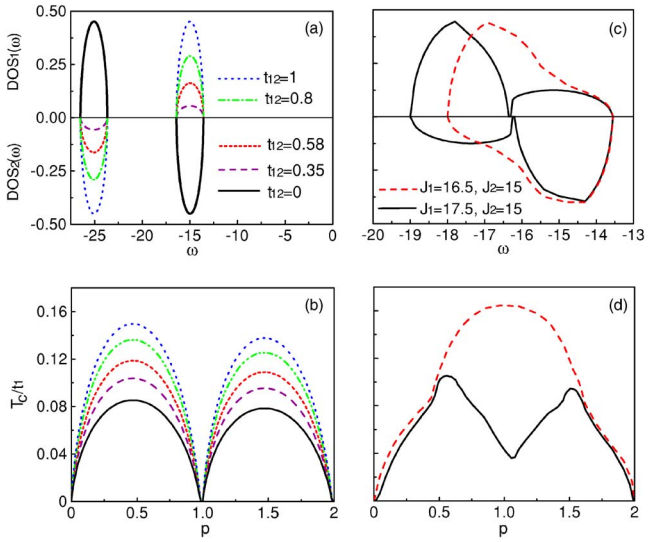

FIG. 1. (Color online) (a) DMFT zero-temperature interacting DOS_l for $J_1=25$ and $J_2=15$ at different t_{12}. (b) T_C vs p for the cases shown in (a). Since the Hund's couplings are very different, the bands and critical temperatures retain the semicircular form. (c) Zero-temperature interacting DOS_l at $t_{12}=0.5$, for the couplings indicated. (d) T_C vs p for the cases shown in (c). Even if the overlap of bands is narrow, the exchange of electrons is strong enough to induce a robust T_C at $p\approx 1$ (solid curve). In all frames $t_1=t_2=1$.

Monte Carlo results. The Hamiltonian (1) is also studied using the MC methods widely applied to Mn oxides in the limit $J\to\infty$ (Ref. 11). Hence, the e_g spins are perfectly aligned with the t_{2g} spin. The technique involves finding the eigenvalues of the Hamiltonian matrix at each MC step corresponding to an updated set of localized spins. Although this substantially limits the size of the clusters being simulated, the results for small lattices are numerically exact and they allow for a direct comparison with DMFT. We simulate lattices of sizes 8^2 in two dimensions and 4^3 in three dimensions. The core spins are treated classically, while the treatment of the fermionic sector is exact. In all simulations 2×10^4 MC steps are used, the first 10^4 being discarded in order to account properly for the thermalization of the random starting configuration. In finite dimensions, the hopping carries a direction index "ξ," that is $t^{\xi}_{ll'}$. In two dimensions (three dimensions), $t^x_l=-\sqrt{3}t^x_{ll'}=-\sqrt{3}t^x_{l'l}=3t^x_{l'}=1$, $t^y_l=\sqrt{3}t^y_{ll'}=\sqrt{3}t^y_{l'l}=3t^y_{l'}=1$, ($t^z_l=t^z_{ll'}=t^z_{l'l}=0, t^z_{l'}=4/3$), in the x, y (and z) directions, respectively.[12] The indexes l and l' stand for the two active x^2-y^2 and $3z^2-r^2$ orbitals. $t_1=1$ sets the energy unit. To find T_C we investigate the long-range spin-spin correlations

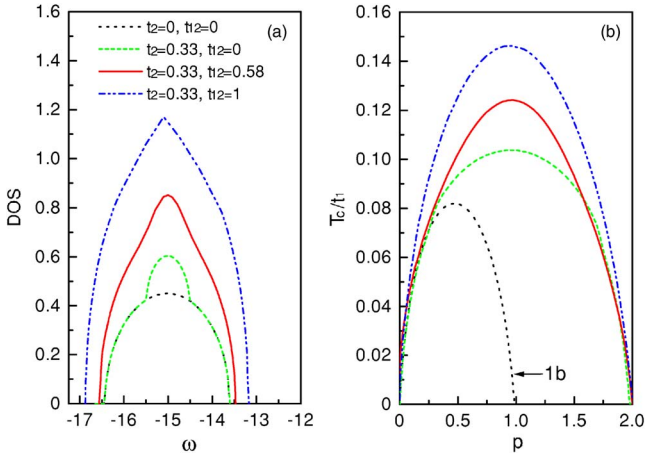

FIG. 2. (Color online) (a) DMFT zero-temperature total interacting DOS for different values of t_{12}. (b) T_C vs p for the parameters indicated in (a). The solid curve corresponds to the realistic set of hoppings (e.g., $LaMnO_3$). In all frames $t_1=1$, $J_1=J_2=15$. The one-band results are also shown (1b).

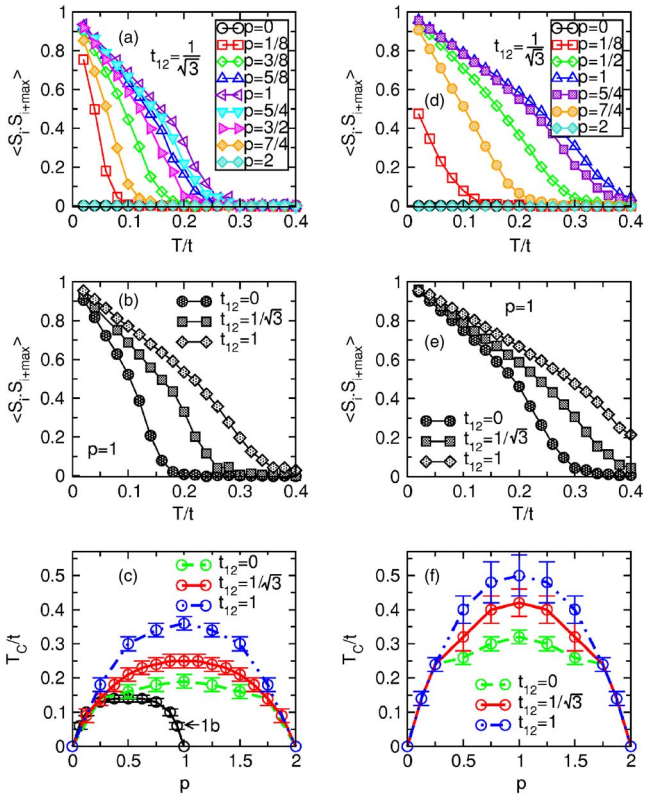

FIG. 3. (Color online) (a) MC spin-spin correlations at $x_{\max}=4\sqrt{2}$ vs temperature for different p, at $t_1=1(\equiv t)$, $t_2=1/3$, and the t_{12} indicated, using an 8^2 lattice. (b) Same as in (a), but changing t_{12}. (c) T_C vs p at different t_{12} for the same lattice used in (a). The one-band results are also shown (1b). The solid curve shows the T_C obtained from (a). (d-f) Same as in (a-c), but using a three-dimensional (3D) lattice of size 4^3. In all frames $J_1=J_2\to\infty$.

$$S(x)=\frac{1}{N}\sum_i\langle\vec{S}_i\cdot\vec{S}_{i+x}\rangle=\frac{1}{N}\sum_i\frac{\mathrm{Tr}(\vec{S}_i\vec{S}_{i+x}e^{-\beta\mathcal{H}})}{\mathrm{Tr}(e^{-\beta\mathcal{H}})},\qquad(6)$$

where N is the total number of sites. T_C is the temperature for which $S\to 0$ upon heating, at the maximum allowed distance $x_{\max}$ in the clusters considered.

In Fig. 3, the results in two and three dimensions are displayed side by side for comparison.[13] Error bars are less than the symbol size unless otherwise indicated. In panel (a), the spin-spin correlations at $x_{\max}$ are shown for an 8^2 lattice, corresponding to different electron densities $p=N_e/N$, where N_e is the total number of electrons. The same in (d), but on a

4^3 lattice. Moreover, we investigate T_C versus p at $t_1=1$, $t_2=1/3$, and different t_{12}. The results are in Fig. 3(b) for two dimensions and in Fig. 3(e) for three dimensions. The T_C is maximum at $p=1$ and vanishes in the limits $p\to 0$ and $p\to 2$, with an overall semicircular form in the phase diagram, as seen in frames (c) and (f). The one-band phase diagram (denoted 1b) is also shown. Hence, as seen in (c) and (f), t_{12} has a substantial effect in raising the T_C, which is in qualitative, and even in quantitative,[14] agreement with DMFT. As t_{12} increases from 0 to 1, the increase in T_C can be as high as 100% in two dimensions and 60% in three dimensions.

The finite-size effects are checked using different boundary conditions and simulating clusters of up to 12^2 in two dimensions and 5^3 in three dimensions. In Fig. 4 the spin-spin correlations at $x_{\max}$ (a) and the magnetization $|M|$ vs T curves (b) are shown. The size effects are small, showing that our MC method detects the T_C accurately.

Conclusion. We carried out a study of a multiband DE model applied to CMR using a powerful combination of DMFT and MC techniques. When two active bands are considered, the T_C is maximized at $p=1$. DMFT shows that the interorbital hopping leads to an increase in T_C at all p's, even if the electron bands do not occupy the same energy interval. This is due to the electron exchange between the bands, which increases the effective number of interacting electrons within each band. Both DMFT and MC indicate that, if the bands fully overlap, besides the increase of T_C due to the energy overlap, a further boost occurs when the interorbital hopping is turned on. The ideas developed here can be used to search for multiorbital FM materials with even higher T_C than currently known, once the off-diagonal hopping is tuned up. Our study can be extended to diluted magnetic semiconductors, with similar results expected.[15]

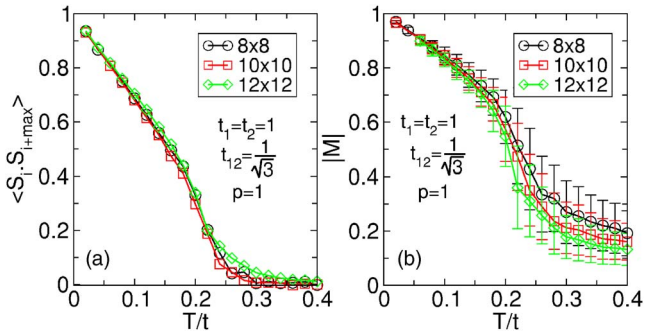

FIG. 4. (Color online) MC finite-size effects studied in two dimensions. (a) Spin-spin correlations at $x_{\max}$ vs temperature for the lattice sizes indicated. (b) $|M|$ vs temperature for the same parameters in (a). The nonzero $|M|$ at high temperatures is the asymptotic $1/\sqrt{N}$ for a system of size N. 3D results using 5^3 lattices are similar (not shown). While the spin-spin correlations do not show appreciable size effects, the magnetization results clearly do, their errors bars being maximal in the critical region.

We acknowledge conversations with R. S. Fishman, J. Moreno, G. Alvarez, A. Moreo, and C. Timm. This research was supported by NSF Grant No. NSF-DMR-0443144.

[1] A. Urushibara, Y. Moritomo, T. Arima, A. Asamitsu, G. Kido, and Y. Tokura, Phys. Rev. B **51**, 14103 (1995); Y. Tokura and N. Nagaosa, Science **288**, 462 (2000).

[2] C. Zenner, Phys. Rev. **82**, 403 (1951); P. W. Anderson and H. Hasegawa, *ibid.* **100**, 675 (1955); P. G. De Gennes, *ibid.* **118**, 141 (1960).

[3] At large J ($\gg 1.4t$) the T_C vs J is almost flat (Ref. 6).

[4] N. Mannella, W. L. Yang, X. J. Zhou, H. Zheng, J. F. Mitchell, J. Zaanen, T. P. Devereaux, N. Nagaosa, Z. Hussain, and Z.-X. Shen, Nature (London) **438**, 474 (2005).

[5] E. Dagotto, New J. Phys. **7**, 67 (2005).

[6] N. Furukawa, J. Phys. Soc. Jpn. **63**, 3214 (1994); **64**, 2754 (1995); **64**, 3164 (1995); cond-mat/9812066 (unpublished).

[7] R. S. Fishman and M. Jarrell, J. Appl. Phys. **93**, 7148 (2003); R. S. Fishman, J. Moreno, Th. Maier, and M. Jarrell, Phys. Rev. B **71**, 180405(R) (2003).

[8] The average $\langle X(\mathbf{m})\rangle = \int d\Omega_{\mathbf{m}} X(\mathbf{m}) P(\mathbf{m})$ is over the orientations $\mathbf{m}$ of the local moment on site 0. $P(\mathbf{m}) \propto \mathrm{Tr}\{\exp[-\mathcal{S}_{\mathrm{eff}}(\mathbf{m})]\}$ is the probability for the local moment to point in the $\mathbf{m}$ direction (one-site probability) and can be obtained by integrating $\exp[-\mathcal{S}_{eff}(\mathbf{m})]$ over the Grassman variables. While $P(\mathbf{m}) = 1/4\pi$ above T_C (Ref. 7), in the FM phase near T_C, $P(\mathbf{m}) \propto \exp(-3\beta T_C M \mathbf{m})$ (Ref. 10), where $\beta = 1/T$ and $M = \langle m_z \rangle_{\mathbf{m}}$ is the local-moment order parameter, nonzero only below T_C.

[9] $\mathrm{DOS}_l(\omega) = -2\,\mathrm{Im}[R_l(\omega)]/\pi$, $\mathrm{DOS}(\omega) = \Sigma_l \mathrm{DOS}_l(\omega)$.

[10] M. Auslender and E. Kogan, Phys. Rev. B **65**, 012408 (2001); E. Kogan and M. Auslender, *ibid.* **67**, 132410 (2003); M. Auslender and E. Kogan, Europhys. Lett. **59**, 277 (2002).

[11] E. Dagotto, *Nanoscale Phase Separation and Colossal Magnetoresistance* (Springer, Berlin, 2003).

[12] J. C. Slater and G. F. Koster, Phys. Rev. **94**, 1498 (1954).

[13] Concerns may arise about a two-dimensional (2D) lattice with a finite T_C, but our MC-simulated 2D system is expected to capture the physics of a real finite 3D system with a nonzero, but very small, coupling in the z direction. This is due to the rapid growth of the correlation length of the 2D system upon cooling (Ref. 11).

[14] With a bandwidth $W=1$ eV at $p=1$, DMFT ($W=4t$), at $J_1=J_2=15$, $t_1 \cong 0.25$ eV, $t_2=t_1/3 \cong 0.083$ eV, $t_{12}=t_1/\sqrt{3} \cong 0.144$ eV, gives $T_C \approx 370$ K, while MC gives in two dimensions ($W=6t$) at $t_1 \sim 0.17$ eV the $T_C \sim 425$ K, and in three dimensions ($W=12t$) at $t_1 \sim 0.084$ eV the $T_C \sim 407$ K.

[15] F. Popescu, Y. Yildirim, G. Alvarez, A. Moreo, and E. Dagotto, Phys. Rev. B **73**, 075206 (2006).